J|A|C|S
ARTICLES

Published on Web 09/18/2009

Decoration of Gold Nanoparticles on Surface-Grown Single-Walled Carbon Nanotubes for Detection of Every Nanotube by Surface-Enhanced Raman Spectroscopy

Haibin Chu,[†,‡] Jinyong Wang,[†] Lei Ding,[‡] Dongning Yuan,[‡] Yan Zhang,[†] Jie Liu,[*,‡] and Yan Li[*,†]

Beijing National Laboratory for Molecular Sciences, State Key Laboratory of Rare Earth Materials Chemistry and Applications, Key Laboratory for the Physics and Chemistry of Nanodevices, College of Chemistry and Molecular Engineering, Peking University, Beijing 100871, China, and Department of Chemistry, Duke University, Durham, North Carolina 27708

Received May 4, 2009; E-mail: yanli@pku.edu.cn; j.liu@duke.edu

Abstract: An electroless deposition method comprised of seed formation and subsequent seeded growth is developed for the decoration of surface-grown single-walled carbon nanotubes (SWCNTs) with gold nanoparticles of controlled size and interparticle distance. The density of the gold nanoparticles is determined by the density of seeds. Gold seeds are used for the SWCNT arrays grown on SiO_x/Si substrates. For the dense SWCNT arrays on quartz, palladium seeds are used because it is much easier to obtain higher quantities of seeds. Attributed to both the seed formation specified on SWCNTs and the succedent efficient seeded growth process, the gold nanoparticles deposit on SWCNTs with very high selectivity. This electroless method shows no selectivity on types, defects, and conductivity of the SWCNTs, and thus ensures the uniform decoration of all SWCNTs on the wafer. Most importantly, this method provides the possibility to realize the optimal configurations of gold nanoparticles on SWCNTs for obtaining maximal surface-enhanced effects and consequently surface-enhanced Raman spectrum (SERS) of each SWCNT. Thus, both the in situ Raman detection of every SWCNT including those nonresonant with laser energy and the observation of the radial breathing modes of SWCNTs originally undetectable with resonance Raman spectroscopy are achieved. Further investigations over the effect of the laser wavelength and the interparticle distance on the SERS enhancement factors of SWCNTs prove that the coupled surface plasmon resonance absorption of the high-density gold nanoparticles decorated on SWCNTs contributes most to the strong surface enhancement.

Introduction

It has long been a big challenge to develop methodologies for detecting the molecular structure and electronic band structure of individual single-walled carbon nanotubes (SWCNTs), especially the surface-grown SWCNTs, which are of great importance in the application of nanoscaled electronics and optoelectronics.[1,2] Rayleigh scattering,[3] electron scattering,[4] and fluorescence spectroscopy[5,6] have shown their partial success in the detection of the (n, m) structure of SWCNTs. However, none of these methods can realize the in situ characterization of all SWCNTs grown on substrates. Resonance Raman spectroscopy (RRS) can probe the structure of SWCNTs at the single tube level.[7−9] However, due to the resonance of excitation photons coinciding with the electronic transition over the band gap of the SWCNTs,[7] the majority of the SWCNTs in a sample cannot be detected using one excitation laser of fixed wavelength or even several wavelengths, especially for the surface-grown SWCNTs, which show relatively low Raman intensity due to the strong interaction between SWCNTs and the substrates.[10,11]

Surface-enhanced Raman spectroscopy (SERS), which typically employs the strong surface plasmon resonance (SPR) of the metal (normally gold or silver) nanoparticles, has succeeded

[†] Peking University.
[‡] Duke University.

(1) Anantram, M. P.; Leonard, F. *Rep. Prog. Phys.* **2006**, *69*, 507–561.
(2) Avouris, P.; Chen, Z. H.; Perebeinos, V. *Nat. Nanotechnol.* **2007**, *2*, 605–615.
(3) Zuo, J. M.; Vartanyants, I.; Gao, M.; Zhang, R.; Nagahara, L. A. *Science* **2003**, *300*, 1419–1421.
(4) Sfeir, M. Y.; Wang, F.; Huang, L. M.; Chuang, C. C.; Hone, J.; O'Brien, S. P.; Heinz, T. F.; Brus, L. E. *Science* **2004**, *306*, 1540–1543.
(5) O'Connell, M. J.; Bachilo, S. M.; Huffman, C. B.; Moore, V. C.; Strano, M. S.; Haroz, E. H.; Rialon, K. L.; Boul, P. J.; Noon, W. H.; Kittrell, C.; Ma, J. P.; Hauge, R. H.; Weisman, R. B.; Smalley, R. E. *Science* **2002**, *297*, 593–596.
(6) Bachilo, S. M.; Strano, M. S.; Kittrell, C.; Hauge, R. H.; Smalley, R. E.; Weisman, R. B. *Science* **2002**, *298*, 2361–2366.
(7) Dresselhaus, M. S.; Dresselhaus, G.; Saito, R.; Jorio, A. *Phys. Rep.* **2005**, *409*, 47–99.
(8) Jorio, A.; Saito, R.; Hafner, J. H.; Lieber, C. M.; Hunter, M.; McClure, T.; Dresselhaus, G.; Dresselhaus, M. S. *Phys. Rev. Lett.* **2001**, *86*, 1118–1121.
(9) Sun, H. D.; Tang, Z. K.; Chen, J.; Li, G. *Appl. Phys. A: Mater. Sci. Process.* **1999**, *69*, 381–384.
(10) Zhang, Y. Y.; Zhang, J.; Son, H. B.; Kong, J.; Liu, Z. F. *J. Am. Chem. Soc.* **2005**, *127*, 17156–17157.
(11) Zhang, Y. Y.; Son, H.; Zhang, J.; Dresselhaus, M. S.; Kong, J.; Liu, Z. F. *J. Phys. Chem. C* **2007**, *111*, 1983–1987.

10.1021/ja9035972 CCC: $40.75

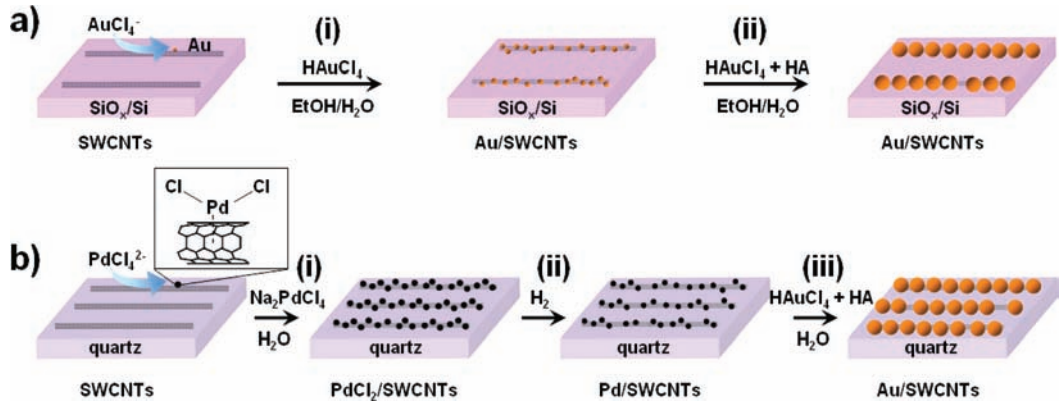

Figure 1. (a) Scheme of the controlled decoration of gold nanoparticles onto SWCNTs based on gold seeds via (i) gold seed decoration and (ii) subsequent seeded growth stages; (b) scheme of the controlled decoration of gold nanoparticles onto SWCNTs based on palladium seeds via (i) $PdCl_2$ adsorption, (ii) H_2 reduction, and (iii) seeded growth stages.

in detecting organic compounds at the single molecule level.[12,13] SERS of SWCNTs both in bulk form[14,15] and grown on surface[16−20] has been studied. However, it remains uncharted and challenging to obtain Raman signals for every SWCNT grown on substrates. Nevertheless, SERS presents a possible approach to probe the structure of all individual SWCNTs because the surface-enhancement effect does not show any selectivity in the electronic transition energy of SWCNTs.[14,21] To achieve this goal, especially to detect the SWCNTs nonresonant with the excitation wavelength, we should focus on obtaining an optimal surface-enhancement effect. First, gold or silver nanoparticles of controlled size and small interparticle distance, which would result in strong coupled SPR absorption with an extraordinary enhancement factor for Raman intensity,[22,23] should be uniformly decorated on every SWCNT. Second, because the SPR absorption and the Raman signals of SWCNTs are strongly polarized,[24,25] three directions, that is, the polarization direction of incident laser, the axis direction of SWCNTs, and the coupled direction of nanoparticles, should be parallel to each other to obtain the strongest Raman signals.

A few methods, including evaporation,[26−28] sputtering, electroless deposition,[16,29−31] and electrochemical deposition,[32−34] have been developed for the decoration of metal nanoparticles on surface-grown SWCNTs. However, the metal nanoparticles decorated via evaporation or sputtering showed poor selectivity on SWCNTs.[26−28] Choi et al. reported that selective electroless metal (gold or platinum) deposition on SWCNTs occurred spontaneously when nanotubes were immersed in corresponding metal salt solutions.[29] Nevertheless, the electroless methods typically resulted in either relatively small metal nanoparticles with sizes normally smaller than the effective SERS diameters of metal nanoparticles[29,30] or low density of metal nanoparticles decorated on SWCNTs.[16] Alternatively, the size and density of metal nanoparticles decorated via electrochemical deposition approaches could be well tuned.[32,34] However, the size and density of metal nanoparticles strongly depended on the conductivity of the SWCNTs and the distance from the electrodes.[20,32] It remains a big challenge to realize the uniform decoration of metal nanoparticles with controlled size and density on every surface-grown SWCNT with high selectivity over the whole wafer.

Here, we report a new electroless approach, which is based on a two-stage deposition process: seed deposition and seeded growth (Figure 1), to decorate highly SERS-active gold nanoparticles of controlled size and interparticle distance on surface-grown SWCNTs. Importantly, the seeds deposit with high selectivity on the sidewalls of SWCNTs via the reduction of $HAuCl_4$ by SWCNTs (Figure 1a), as reported by Choi et al.,[29] or the formation of stable complexes between $PdCl_2$ and SWCNTs (Figure 1b). Moreover, the well-controlled seeded growth ensures the selective decoration of gold nanoparticles with controlled size and interparticle distance on SWCNTs.

(12) Kneipp, K.; Wang, Y.; Kneipp, H.; Perelman, L. T.; Itzkan, I.; Dasari, R.; Feld, M. S. *Phys. Rev. Lett.* **1997**, *78*, 1667–1670.
(13) Kneipp, K.; Kneipp, H.; Kneipp, J. *Acc. Chem. Res.* **2006**, *39*, 443–450.
(14) Kneipp, K.; Kneipp, H.; Corio, P.; Brown, S. D. M.; Shafer, K.; Motz, J.; Perelman, L. T.; Hanlon, E. B.; Marucci, A.; Dresselhaus, G.; Dresselhaus, M. S. *Phys. Rev. Lett.* **2000**, *84*, 3470–3473.
(15) Kneipp, K.; Kneipp, H.; Dresselhaus, M. S.; Lefrant, S. *Philos. Trans. R. Soc. London, Ser. A* **2004**, *362*, 2361–2373.
(16) Mieszawska, A. J.; Jalilian, R.; Sumanasekera, G. U.; Zamborini, F. P. *J. Am. Chem. Soc.* **2005**, *127*, 10822–10823.
(17) Assmus, T.; Balasubramanian, K.; Burghard, M.; Kern, K.; Scolari, M.; Fu, N.; Myalitsin, A.; Mews, A. *Appl. Phys. Lett.* **2007**, *90*, 173109.
(18) Chen, Y. C.; Young, R. J.; Macpherson, J. V.; Wilson, N. R. *J. Phys. Chem. C* **2007**, *111*, 16167–16173.
(19) Scolari, M.; Mews, A.; Fu, N.; Myalitsin, A.; Assmus, T.; Balasubramanian, K.; Burghard, M.; Kern, K. *J. Phys. Chem. C* **2008**, *112*, 391–396.
(20) Huang, S. M.; Qian, Y.; Chen, J. Y.; Cai, Q. R.; Wan, L.; Wang, S.; Hu, W. B. *J. Am. Chem. Soc.* **2008**, *130*, 11860.
(21) Takagi, D.; Homma, Y.; Hibino, H.; Suzuki, S.; Kobayashi, Y. *Nano Lett.* **2006**, *6*, 2642–2645.
(22) Schuck, P. J.; Fromm, D. P.; Sundaramurthy, A.; Kino, G. S.; Moerner, W. E. *Phys. Rev. Lett.* **2005**, 94.
(23) Xu, H. X.; Aizpurua, J.; Kall, M.; Apell, P. *Phys. Rev. E* **2000**, *62*, 4318–4324.
(24) Luo, W.; van der Veer, W.; Chu, P.; Mills, D. L.; Penner, R. M.; Hemminger, J. C. *J. Phys. Chem. C* **2008**, *112*, 11609–11613.
(25) Duesberg, G. S.; Loa, I.; Burghard, M.; Syassen, K.; Roth, S. *Phys. Rev. Lett.* **2000**, *85*, 5436–5439.
(26) Kong, J.; Chapline, M. G.; Dai, H. J. *Adv. Mater.* **2001**, *13*, 1384–1386.
(27) Li, Y. M.; Kim, W.; Zhang, Y. G.; Rolandi, M.; Wang, D. W.; Dai, H. J. *J. Phys. Chem. B* **2001**, *105*, 11424–11431.
(28) Kumar, R.; Zhou, H.; Cronin, S. B. *Appl. Phys. Lett.* **2007**, *91*, 223105.
(29) Choi, H. C.; Shim, M.; Bangsaruntip, S.; Dai, H. J. *J. Am. Chem. Soc.* **2002**, *124*, 9058–9059.
(30) Lee, Y.; Song, H. J.; Shin, H. S.; Shin, H. J.; Choi, H. C. *Small* **2005**, *1*, 975–979.
(31) Qu, L. T.; Dai, L. M. *J. Am. Chem. Soc.* **2005**, *127*, 10806–10807.
(32) Day, T. M.; Unwin, P. R.; Wilson, N. R.; Macpherson, J. V. *J. Am. Chem. Soc.* **2005**, *127*, 10639–10647.
(33) Fan, Y. W.; Goldsmith, B. R.; Collins, P. G. *Nat. Mater.* **2005**, *4*, 906–911.
(34) Quinn, B. M.; Dekker, C.; Lemay, S. G. *J. Am. Chem. Soc.* **2005**, *127*, 6146–6147.

Besides, the nanoparticles align well along the SWCNTs, making it easy for alignments with the incident laser polarization. As a result, our method not only lights up all SWCNTs using only one excitation laser wavelength, but also enables the observation of radial breathing mode (RBM) peaks originally undetectable with RRS.

Experimental Methods

Decorating Gold Nanoparticles onto SWCNTs by Seeded Growth Based on Gold Seeds. The gold/SWCNT composites were prepared by an electroless deposition method comprised of a two-stage process: seed deposition and seeded growth (Figure 1a). Horizontally aligned SWCNTs were grown on either quartz or SiO_x/Si substrates as previously reported.[35−39] The as-grown SWCNT samples were first immersed into a 5 mM $HAuCl_4$ ethanol/water (1/1, v/v) solution for 5 min to deposit gold seeds, then rinsed with ethanol and water. This step was repeated once again to increase the density of gold seeds on SWCNTs. Next, the samples were immersed into a seeded growth solution containing 0.05 mM $HAuCl_4$ and 0.25 mM hydroxylamine hydrochloride (HA) in ethanol/water (1/1, v/v) for 1 h, followed by rinsing with ethanol and water.

Decorating Gold Nanoparticles onto SWCNTs by Seeded Growth Based on Palladium Seeds. The gold/SWCNT composites were prepared by an electroless method comprised of a three-stage process: $PdCl_2$ adsoprtion, H_2 reduction, and seeded growth (Figure 1b). High-density arrays of horizontally aligned SWCNTs were grown on quartz, as previously reported.[38,39] The as-grown SWCNT samples were first immersed into a 5 mM Na_2PdCl_4 solution for several minutes to deposit $PdCl_2$ nanoparticles, then rinsed with water. The samples were then transferred into a quartz tube and reduced by H_2 for 10 min at room temperature. Finally, the samples were immersed into a seeded growth solution containing 0.25 mM $HAuCl_4$ and 0.25 mM HA, followed by rinsing with water.

Characterizations. The obtained products were characterized via SEM (FEI XL30 SEM-FEG), AFM (Seiko SPA400 or Veeco Nanoscope IIIa, at tapping mode), absorption spectrometer (Perkin-Elmer Lambda 35), Raman spectrometer (Horiba LabRam ARAMIS or LabRam HR 800), XRD (Rigaku Dmax-2000 with Cu Kα radiation, $\lambda = 1.5406$ Å), and XPS (Kratos Axis Ultra). Raman spectra were taken after aligning the axis of the SWCNTs along the laser polarization direction under the optical microscope attached to the Raman spectrometer. The typical spot size of the laser was around 1 μm under a 100× objective lens, and the laser energy was carefully controlled to avoid any heat effect (typically about 1.2 mW).

Results and Discussion

1. Selective Electroless Deposition of Gold Nanoparticles on Surface-Grown SWCNTs Based on Gold Seeds. For the SWCNT arrays grown on SiO_x/Si substrates, we used gold seeds to grow dense gold nanoparticles (Figure 1a). It was found that the seeds were selectively deposited on SWCNTs and the density could be controlled (Figure S1 in the Supporting Information). Figure 2a and b shows typical SEM images of SWCNTs on SiO_x/Si before and after gold decoration, respectively. Uniform gold nanoparticles with the size of 147 ± 23 nm (Figure 2c)

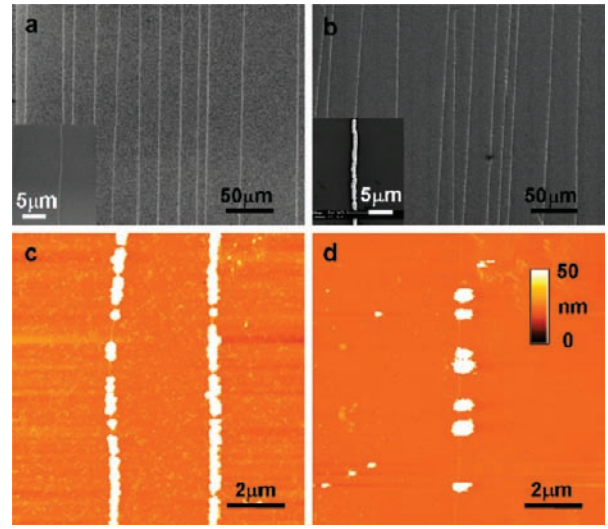

Figure 2. (a) SEM image of the as-grown SWCNTs on SiO_x/Si; the inset is the magnified image; (b) SEM image after gold decoration via gold seed mediated growth; the inset is the magnified image; (c) AFM topographical image of the gold/SWCNT composites obtained after seeded growth in 0.05 mM $HAuCl_4$ + 0.25 mM HA; (d) AFM image after seeded growth in 0.25 mM $HAuCl_4$ + 0.25 mM HA.

and a density of 3−4 nanoparticles per micrometer of SWCNT (NPs/μm SWCNT) were selectively formed on SWCNTs after gold seed deposition and subsequent seeded growth. The average interparticle distance of the adjacent gold nanoparticles was about 140 nm. Importantly, due to the selective nucleation of gold seeds on the sidewalls of SWCNTs via the reaction between $HAuCl_4$ and SWCNTs,[27,29] almost all of the gold nanoparticles were decorated on SWCNTs. Moreover, both the size and the density of gold nanoparticles could be tuned. The density of gold seeds could be tuned from 3 to over 30 NPs/μm SWCNT (Figure S1 in the Supporting Information) by adjusting the reaction time and repetition times during the seed deposition stage; the diameter (D) of the final gold particles on SWCNTs could easily be altered from several to hundreds of nanometers (Figure S2 in the Supporting Information) by increasing the seeded growth time. As a result, the interparticle distance (d) decreases rapidly from about 500 to 17 nm with the elongation of seeded growth time (Figure S2 in the Supporting Information). Other experimental parameters, such as the ethanol/water ratio during the seed deposition, and the reactant concentrations in the seeded growth stage could also help to tune the diameter and interparticle distance of the final gold nanoparticles on SWCNTs. For instance, from far separated gold nanoparticles with interparticle distance over 1 μm and a d/D value of about 5 (Figure 2d) to continuous gold nanowires (inset in Figure 2b and Figure S2c in the Supporting Information) can all be formed by varying the reaction conditions.

2. Controlled Decoration of Gold Nanoparticles on Surface-Grown Dense SWCNTs Based on Palladium Seeds. Gold-seeded growth showed extremely high selectivity on nanotubes for SWCNT arrays on SiO_x/Si substrates and obtained high-density nanoparticles deposited only on SWCNTs. It showed even higher selectivity of nanoparticle deposition on tubes for the dense SWCNT arrays grown on quartz wafers, but the density of the deposited particles was found to be relatively low (Figures 3). One of the reasons may be the relative low seed formation efficiency of gold on dense SWCNT arrays. Thus, we exploited another process based on palladium seeds for the high-density SWCNT arrays (Figure 1b and Figure S3

(35) Zhou, W. W.; Han, Z. Y.; Wang, J. Y.; Zhang, Y.; Jin, Z.; Sun, X.; Zhang, Y. W.; Yan, C. H.; Li, Y. *Nano Lett.* **2006**, *6*, 2987–2990.
(36) Jin, Z.; Chu, H. B.; Wang, J. Y.; Hong, J. X.; Tan, W. C.; Li, Y. *Nano Lett.* **2007**, *7*, 2073–2079.
(37) Zhang, Y.; Zhou, W. W.; Jin, Z.; Ding, L.; Zhang, Z. Y.; Liang, X. I.; Li, Y. *Chem. Mater.* **2008**, *20*, 7521–7525.
(38) Ding, L.; Yuan, D. N.; Liu, J. *J. Am. Chem. Soc.* **2008**, *130*, 5428–5429.
(39) Ding, L.; Tselev, A.; Wang, J. Y.; Yuan, D. N.; Chu, H. B.; McNicholas, T. P.; Li, Y.; Liu, J. *Nano Lett.* **2009**, *9*, 800–805.

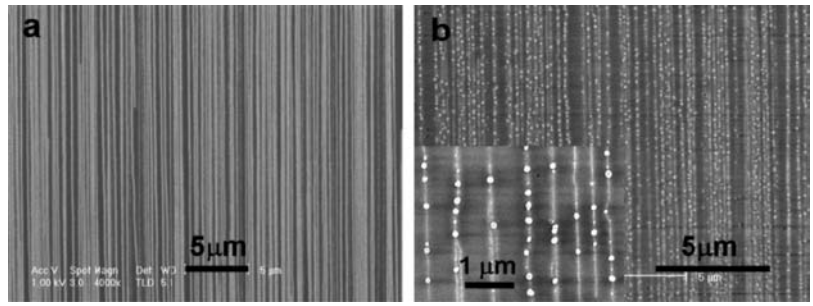

Figure 3. SEM images of the high-density SWCNT arrays on quartz (a) before and (b) after gold decoration based on gold seeds via repeating both the gold seed deposition process and the seeded growth process several times. Inset of (b) is the magnified image.

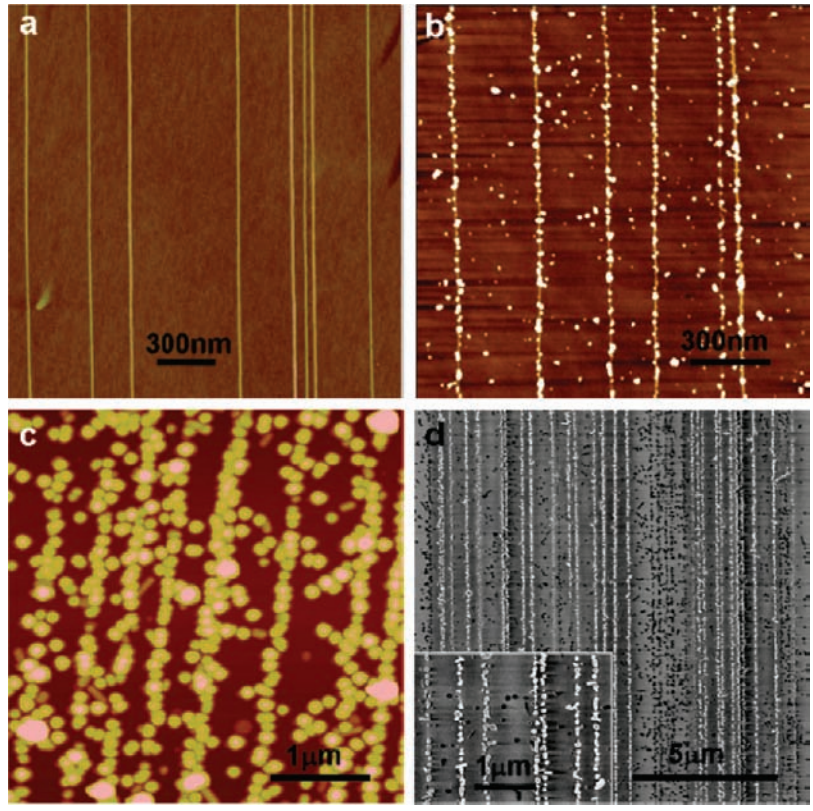

Figure 4. AFM topographical images of (a) the as-grown high-density SWCNT arrays on quartz and (b) the $PdCl_2$/SWCNT composites. (c) AFM topographical image and (d) SEM image of the gold/SWCNT composites obtained by seeded growth based on palladium seeds. Inset in (d) is the magnified image.

of the Supporting Information). From an organometallic chemical point of view, it is possible to form rather stable d−π complexes of $PdCl_2$ with the sidewalls of carbon nanotubes when exposing SWCNTs in the solution of Na_2PdCl_4.[40−42] As shown in Figure 4b, after being immersed in 5 mM Na_2PdCl_4 solution for 2 min, $PdCl_2$ nanoparticles with a uniform size of 6.8 ± 1.8 nm and a high density of over 30 NPs/μmSWCNT were chemically adsorbed on SWCNTs. The nanoparticles were then reduced by H_2 to Pd with a smaller size of 5.7 ± 1.8 nm and a lower density of about 25 NPs/μm SWCNT. The Pd nanoparticles were used as the seeds for further gold deposition, resulting in gold nanoparticles with a size of 54.7 ± 8.5 nm and a high density of about 12 NPs/μm SWCNT (Figure 4c and d). The average interparticle distance of the adjacent gold nanoparticles was smaller than 30 nm, which was smaller than the size of nanoparticles. Here, ~85% of the nanoparticles were deposited on SWCNTs. It is not as high as that in the gold-seeded process; however, it is still satisfying. The size and density of the deposited particles could also be well controlled (Figures S4, S5, and S6 in the Supporting Information). For example, when the adsorption time in the seed deposition step was adjusted from 1 to 3 min, the size of the gold nanoparticles decreased from 88 ± 35 to 32 ± 11 nm, while the density of gold nanoparticles increased from 3 to 13 NPs/μm SWCNT, and thus the average interparticle distance decreased from 245 to 42 nm.

3. In Situ SERS Measurement of Every Individual SWCNT on Substrates. As shown above, gold nanoparticles with well-controlled size and small interparticle distance can be decorated uniformly on all SWCNTs with our methods. The nanoparticles

(40) King, R. B., Ed. *Encyclopedia of Inorganic Chemistry*; John Wiley & Sons: West Sussex, 1994; Vol. 6.
(41) Simonov, P. A.; Troitskii, S. Y.; Likholobov, V. A. *Kinet. Catal.* **2000**, *41*, 255–269.
(42) Simonov, P. A.; Romanenko, A. V.; Prosvirin, I. P.; Moroz, E. M.; Boronin, A. I.; Chuvilin, A. L.; Likholobov, V. A. *Carbon* **1997**, *35*, 73–82.

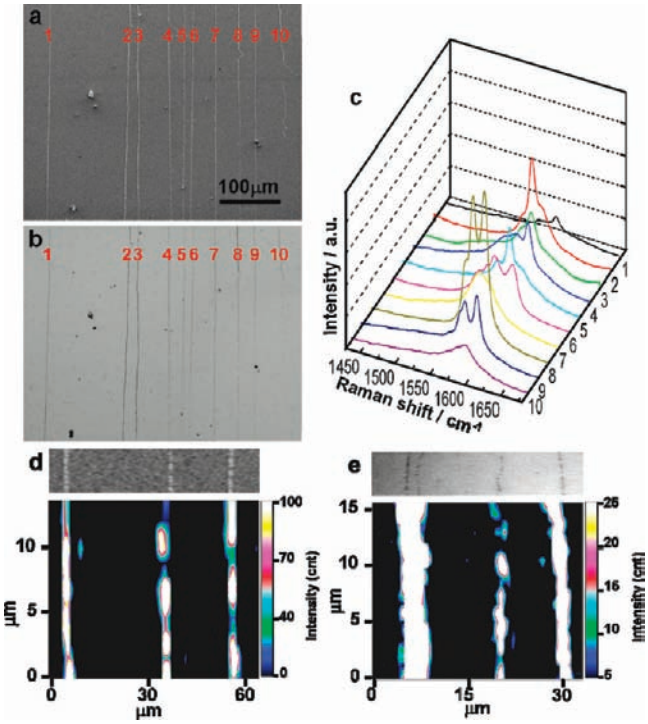

Figure 5. SEM image (a), optical image (b), and corresponding Raman spectra (c) of 10 SWCNTs grown on SiO_x/Si after gold decoration with an excitation wavelength of 633 nm. Mapping of the Raman intensity of three SWCNTs (d) and four SWCNTs (e), respectively, in the range of 1450−1650 cm^{-1} with the corresponding SEM image (d) and optical image (e) shown above. The distance between the left two SWCNTs in (e) (~1.5 μm) is smaller than twice the laser spot diameter ($2d \approx 2$ μm), and hence these two SWCNTs overlapped in the mapping image.

align well along the SWCNTs. This kind of structure ensures the strong SPR absorption, which will result in large SERS enhancement for SWCNTs. In addition, all of the SWCNTs become visible under optical microscope after gold decoration (Figure 5a and b). This also facilitates the achievement of strong Raman signal of SWCNTs attributed to the convenience in aligning the SWCNTs to the incident laser polarization direction.[25]

It was found in our experiments that for the as-grown SWCNTs on SiO_x/Si wafers,[35−37] only about one-third of the SWCNTs showed detectable Raman signal using the excitation wavelength of 633 nm. This indicated that the other two-thirds of the SWCNTs were not in resonance with 633 nm laser. We then measured the Raman spectra of nanotubes in a gold-decorated sample of about 200 horizontally aligned SWCNTs grown on a 1 × 1 cm^2 SiO_x/Si wafer. It was gratifying to find that the G-band (tangential mode) signals of all of the SWCNTs on the wafer were observed after gold decoration. Figure 5a and b shows the SEM and the corresponding optical image of the representative 10 SWCNTs whose Raman spectra are shown in Figure 5c. The lighting up of every SWCNT was further confirmed by the mapping of the intensity from the G-bands of SWCNTs (Figure 5d and e).

Because of its narrow resonance windows, RBM peaks of nonresonant SWCNTs are especially difficult to be obtained using RRS.[7] However, the high SERS-active gold nanoparticles decorated on SWCNTs not only render the full emerging of the G-bands of all SWCNTs, but also enable the observation of the RBM peaks originally undetectable with RRS. Figure 6a−d shows the typical Raman spectra of the nearly pure semiconducting SWCNT sample on quartz[39] before and after gold decoration. The aligned SWCNTs have a narrow diameter distribution of 1.5−1.8 nm with more than 95% nanotubes being semiconducting,[39] which were theoretically not resonant with 785 nm laser energy.[7] No RBM peak was observed before gold decoration (Figure 6a), and the G-band was also difficult to detect. However, nearly all of the SWCNTs showed obvious RBM bands and strong G-bands after gold decoration. For instance, a strong RBM peak with frequency ω_{RBM} around 160 cm^{-1} appeared after gold decoration (Figure 6a). This peak was assigned to SWCNTs with a diameter d_t of 1.55 nm, by the relation $d_t = 248/\omega_{RBM}$.[7] The appearance of the G^- peak around 1575 cm^{-1}, the low intensity ratio of G^- to G^+, and the absence of the Breit−Wigner−Fano (BWF) peak within the G line (Figure 6b) indicated the SWCNT is semiconducting. The appearance of RBM peak around 160 cm^{-1} resulted from the nonresonant SERS of the SWCNTs decorated with the high SERS-active gold nanoparticles. The observation of the RBM peaks originally undetectable with RRS further confirmed the strong SERS enhancement of the nonresonant SWCNTs with the excitation wavelength of 785 nm. The same SWCNT sample was also investigated by 633 nm laser, with whose energy these semiconducting SWCNTs were in resonance. Both the intensity of the RBM (Figure 6c) and the G-band (Figure 6d) increased significantly after gold decoration.

4. Mechanism for Strong Surface Enhancement Effects of Closely Packed Gold Nanoparticles. Figure 7a and Table S1 compared the apparent SERS enhancement strength for G-band intensity of SWCNTs with different excitation wavelengths. More than 10 spectra were taken with each laser wavelength before and after gold decoration. The average apparent SERS enhancement factors of G-band intensity after gold decoration are 6.4, 54, and 97 upon excitation with laser wavelengths of 442, 633, and 785 nm, respectively. Also, the maximum apparent enhancement factors are 14.8, 186, and 629 upon excitation with laser wavelengths of 442, 633, and 785 nm, respectively. From the results, we can find that the enhancement strength is excitation wavelength dependent. The absorption spectra of the gold nanoparticle-decorated SWCNTs grown on quartz were then measured to deduce the origin of this phenomenon. As shown in the absorption spectrum (Figure 7b), the as-fabricated gold/SWCNT composites display a narrow plasmon band at ~500 nm, and a broad and intense plasmon band in the near-infrared region. These two bands arise from the SPR of individual gold nanoparticles and the coupled SPR of the adjacent gold nanoparticles with small gaps, respectively.[43,44] The total SPR absorbance decreases at the sequence of 785 > 633 > 442 nm, which mainly attributes to the decreasing coupled SPR absorbance.[44,45] This results in the stronger enhancement of Raman intensity with 633 nm laser and 785 nm laser than that with 442 nm laser (Figure 7b).

Additionally, the enhancement factors were found to be much larger in areas with adjacent gold nanoparticles (interparticle distance smaller than 10 nm, d/D value smaller than 0.1) than in areas with far separated gold nanoparticles (interparticle distance larger than 1 μm, d/D value about 5), as shown in Figure 8. Previous theoretical and experimental results showed that the electromagnetic coupling of metal nanoparticles be-

(43) Ghosh, S. K.; Pal, T. *Chem. Rev.* **2007**, *107*, 4797–4862.
(44) Wang, H.; Levin, C. S.; Halas, N. J. *J. Am. Chem. Soc.* **2005**, *127*, 14992–14993.
(45) Jain, P. K.; Huang, W. Y.; El-Sayed, M. A. *Nano Lett.* **2007**, *7*, 2080–2088.

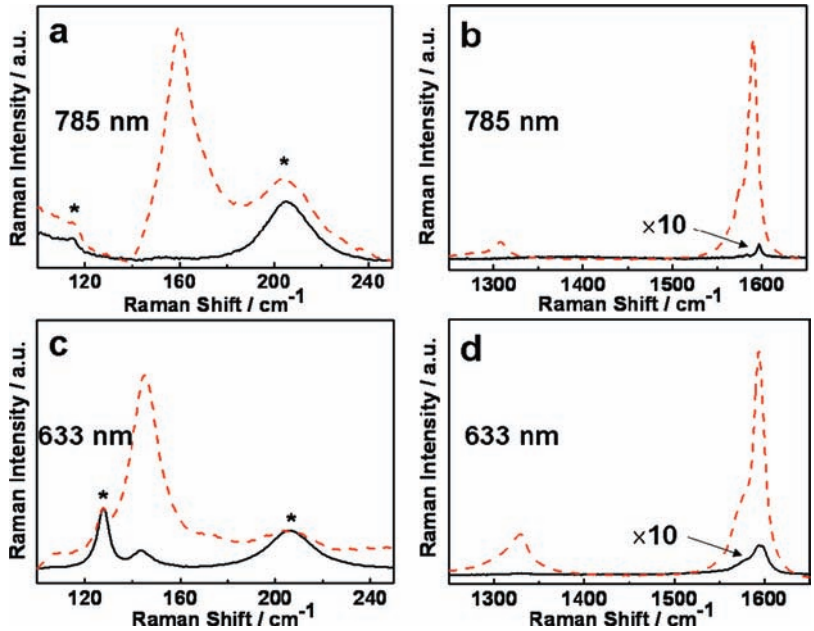

Figure 6. Raman spectra of nearly pure semiconducting SWCNTs before (black solid curves) and after (red dotted curves) gold nanoparticles' decoration under different laser excitation. (a,b) 785 nm laser, the same nanotube. (c,d) 633 nm laser, another nanotube. All of the spectra were normalized to the quartz substrate peak at around 464 cm^{-1}. The peaks marked with an asterisk arise from the quartz substrate.

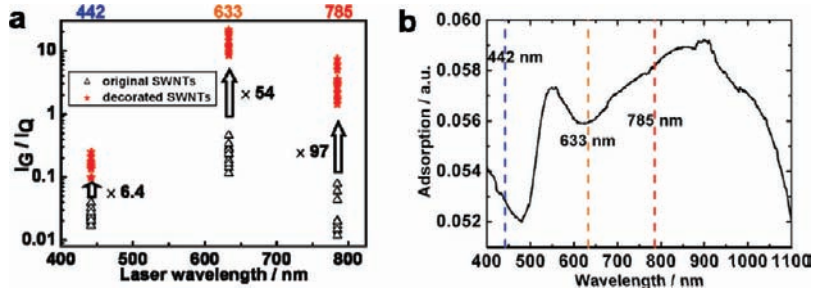

Figure 7. (a) Different apparent SERS enhancement factors for intensity of G^+ peaks of SWCNTs with different excitation wavelength. I_Q is the intensity of typical Raman peak of quartz at around 464 cm^{-1}. (b) Vis−NIR absorption spectrum of the gold/SWCNT composites on quartz.

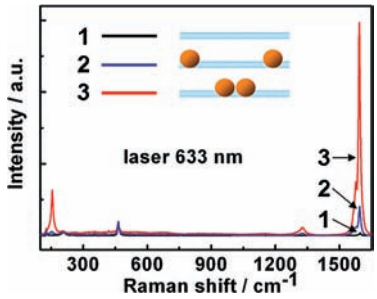

Figure 8. The effect of interparticle distance on SERS enhancement factor. The adjacent gold nanoparticles (interparticle distance <10 nm) increased the intensity of the G^+ peak by 108 times, while the far separated gold nanoparticles (interparticle distance >1 μm) only increased the intensity of the G^+ peak by 13 times.

comes effective when the interparticle distance is smaller than about 2.5 times the particle diameter ($d/D \leq 2.5$).[43,46] Also, the electromagnetic SERS enhancement factor increases approximately exponentially with decreasing interparticle distance.[23,24] Therefore, it further confirmed that the strong SERS enhancement of SWCNTs mainly came from the electromagnetic SERS enhancement caused by the coupled SPR absorption of decorated gold nanoparticles with high density and small interparticle distance.

Actually, the enhancement factors shown in Figure 7a and Table S1 do not represent the real enhancement strength for nonresonant SWCNTs. When we made the statistical analysis, only the band intensities of resonant SWCNTs before gold decoration were used because the nonresonant tubes do not give any Raman signal before gold decoration. The real enhancement factors for nonresonant tubes should be much higher than those shown in Figure 7a and Table S1; otherwise, it should be still infeasible to observe the Raman spectra of the nonresonant SWCNTs after gold decoration under an enhancement of only several hundred times. As claimed in the previous report about the bulk SWCNTs,[14] the SERS enhancement factors could be as large as 10^{12}. This may be a reference for us to make a rough prediction about the magnitude of the SERS enhancement factor of surface-grown SWCNTs.

5. Do the SERS Results Reflect the Intrinsic Properties of All SWCNTs in a Sample? Another question that arises is whether the SERS gives a reliable measurement of the intrinsic properties of all SWCNTs in a sample. From the work of Collin's group, the electro-deposited gold nanoparticles tended to nucleate at defect sites on nanotubes.[33] However, as already

(46) Su, K. H.; Wei, Q. H.; Zhang, X.; Mock, J. J.; Smith, D. R.; Schultz, S. *Nano Lett.* **2003**, *3*, 1087–1090.

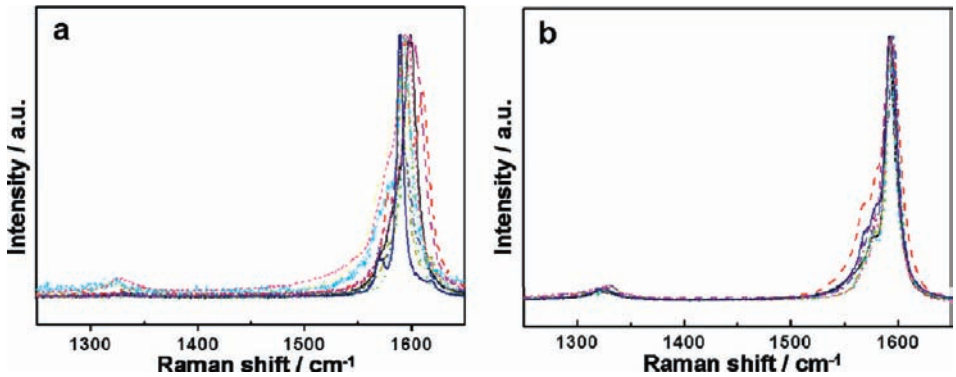

Figure 9. Raman spectra of the D- and G-bands of the SWCNTs grown on quartz substrates (a) before and (b) after decoration of the gold nanoparticles under the 633 nm laser excitation. All of the spectra were normalized to the G^+ peaks.

mentioned above, our electroless method ensures the uniform decoration of high density gold nanoparticles on all SWCNTs. The density can be higher than 10 NPs/μm SWCNT, which is much higher than the defect density of the surface-grown SWCNTs produced by chemical vapor deposition method (typically less than one defect per micrometer of SWCNT).[33] This indicates that our electroless method shows no decorating selectivity on defects, types, and conductivity of the SWCNTs. Therefore, we can obtain the SERS of each SWCNT in a sample.

It is reported that SERS is not stable in some cases due to the blinking effect.[12,47] The origin of the blinking effect is still unclear. Some people ascribed it to the thermal effect of the molecules adsorbed on metal nanoparticles.[48] In our experiments, the blinking effect was found to be rather weak for SERS of SWCNTs after gold decoration. Both the signal intensities and the frequencies did not change much in several minutes (Figure S8). One of the reasons may be the low laser power (typically about 1.2 mW) we used for taking the Raman spectra. The blinking effect did not become obvious until the laser power was above 3 mW.

Furthermore, the peak intensity ratio of the D-band over that of the G-band of the SWCNTs, I_D/I_G, did not change much before ($I_D/I_G = 0.02-0.08$) and after gold decoration ($I_D/I_G = 0.03-0.07$) in our method from the statistics of almost all spectra we obtained. Some of these spectra are typically shown in Figure 9. This reveals that our electroless method did not generate new defects during gold decoration of the SWCNTs. Besides, the oxidation state of the gold was determined by XPS as shown in Figures S3c and S3d. The XPS spectra of the gold nanoparticles decorated on SWCNTs show the Au $4f_{7/2}$ and Au $4f_{5/2}$ doublet with the binding energies of 84.2 and 87.9 eV, which are typical values of Au^0.[49] This indicates the charge transfer between SWCNTs and gold nanoparticles is weak, which has a small effect on the intrinsic properties of SWCNTs.[19] Thus, the SERS achieved in our method reflects the intrinsic properties of the SWCNTs.

Conclusions

In summary, an electroless deposition method comprised of seed deposition and seeded growth has been developed to decorate surface-grown SWCNTs with gold nanoparticles with controlled size and high density, consequentially of high SERS activity for lighting up all SWCNTs including those nonresonant with laser photon energy. The strong SERS enhancement mainly comes from the electromagnetic SERS attributed to the coupled SPR absorption in the high density gold nanoparticles aligned on SWCNTs. This SERS method could potentially be developed into a metrological tool for in situ characterization of all SWCNTs with only one laser wavelength. Also, it would be the third technique after Rayleigh scattering and electron scattering that can be used for the full detection of each individual SWCNT in a sample and the only method to in situ characterize every SWCNT on substrates. Possibly, the aligned gold nanoparticle/SWCNT composites can find more applications such as polarizers in optical devices.

Acknowledgment. The work performed at Peking University was supported by the NSF (Projects 50772002 and 90406018) and MOST (Projects 2006CB932403, 2007CB936202, and 2006CB932701) of China. The work performed at Duke University is supported by the NRL (N00173-04-1-G902) and a fund from Duke University. We would like to thank Dr. Alvin L. Crumbliss and Esther Tristani at Duke University for helpful discussions. H.C. would like to thank the China Scholarship Council and Duke University for supporting his study at Duke.

Supporting Information Available: Characterization details, more figures of the controlled decoration of gold nanoparticles onto SWCNTs, detailed analysis of the origin of the SERS enhancement, and different SERS enhancement factors of SWCNTs' G-band intensity with different excitation wavelength. This material is available free of charge via the Internet at http://pubs.acs.org.

JA9035972

(47) Nie, S. M.; Emory, S. R. *Science* **1997**, *275*, 1102–1106.
(48) Maruyama, Y.; Ishikawa, M.; Futamata, M. *J. Phys. Chem. B* **2004**, *108*, 673–678.
(49) Hu, X. G.; Wang, T.; Qu, X. H.; Dong, S. J. *J. Phys. Chem. B* **2006**, *110*, 853–857.